Available online at www.sciencedirect.com

ScienceDirect

journal homepage: www.elsevier.com/locate/issn/15375110

Research Paper

Media filter fouling assessment using optical coherence tomography: New methodology

Miquel Duran-Ros [a,*], Carles Solé-Torres [a], Nassim Ait-Mouheb [b], Bruno Molle [b], Gerard Arbat [a], Jaume Puig-Bargués [a]

[a] Department of Chemical and Agricultural Engineering and Technology, University of Girona, Carrer Maria Aurèlia Capmany, 61, 17003, Girona, Catalonia, Spain

[b] INRAE, UMR GEAU, University of Montpellier, Montpellier, France

ARTICLE INFO

Article history:
Received 25 September 2020
Received in revised form
7 January 2021
Accepted 9 January 2021
Published online 29 January 2021

Keywords:
Filtration
Particle removal
Clogging
Image analysis
Drip irrigation
Reclaimed wastewater reuse

Drip irrigation is an efficient and safe system for reusing wastewater in agriculture. Since emitter clogging is its main limitation, filtration is needed for preventing it. Media filters are commonly used when irrigation water has a high particle load. However, particle removal through a media bed in media filters used in drip irrigation systems has not been widely studied mainly due to experimental difficulties. To overcome this issue a new methodology using optical coherence tomography (OCT) is presented here. Experiments were carried out on a media filter at laboratory scale using wastewater. Once the filter was clogged, several 20 mm slices were taken and the retained total suspended solids were analysed by gravimetry. Following this, particles retained at six different locations of each slice were also determined using OCT. Results show a good agreement between total suspended solids experimentally determined and particles determined with OCT, especially when pixels attributed to particles were 30–45% of the total. Therefore, OCT could be a useful technique for assessing particle retention at different media depths.

1. Introduction

Good agricultural practices, consistent irrigation management and efficient treatments that limit the impact of wastewater reuse on the environment (Lazarova & Bahri, 2004; Ait-Mouheb et al., 2018) make it possible to reserve good quality water for more sensitive uses such as drinking water. Drip irrigation improves water use efficiency (Ayars et al., 2007) and allows a safe use of reclaimed wastewater (RWW) (WHO, 2006). However, emitter clogging is a major issue (Nakayama et al., 2007, Lequette, Ait-Mouheb, Wery, 2020) since it disturbs operation, reduces distribution uniformity and longevity and this can affect the economic competitiveness of drip irrigation systems (Lamm & Rogers, 2017). Irrigation water filtration is a key maintenance practice for preventing emitter clogging (Nakayama et al., 2007). Media filters are an effective option (Trooien & Hills, 2007) especially when reclaimed effluents are used thanks to its ability in removing suspended solids (Puig-Bargués et al., 2005). Media filters used in drip irrigation are usually pressurised vertical cylindrical tanks, where packed sand is used as filtering media (Burt & Styles, 2016). Solé-Torres et al. (2019) pointed out that a

* *Corresponding author*. Fax: +34 972418399.
E-mail address: miquel.duranros@udg.edu (M. Duran-Ros).
https://doi.org/10.1016/j.biosystemseng.2021.01.008

Nomenclature

COD	Chemical oxygen demand (g m^{-3})
d_e	Effective diameter (mm)
OCT	Optical coherence tomography (–)
$P_{fouling}$	Number of pixels corresponding to retained particles from OCT acquisitions (pixels)
$P_{measurement\ zone}$	Number of pixels of total OCT acquisitions of the sample determined by the taken image (pixels)
PMMA	Polymethyl methacrylate (–)
TSS	Total suspended solids (mg l^{-1})
RMSE	Root mean square error (–)
RWW	Reclaimed wastewater (–)

deeper understanding of the performance of pressurised media filters is needed for irrigation engineers and practitioners to achieve efficient design and management of this irrigation equipment. This knowledge should be focused on determining the behaviour of removal efficiency across the porous media bed to better understand the phenomena involved and their mechanisms.

When water is forced to pass through the porous media bed, those particles carried by irrigation water are retained on the media and, consequently, head loss across the filter increases over time (EPA, 1995; Awady et al., 2008). This head loss, which also depends on the superficial water filtration velocity (i.e. water flow rate per filter surface area) and filter media size, progressively increases until the filter becomes completely fouled, a condition in which solids are no longer removed by the already over-loaded filter (EPA, 1995). Some studies have focused on trying to explain the effect of filtration velocity and media size on total head loss or on particle removal achieved by the filter. Thus, Mesquita et al. (2019) reported that the removal efficiency of a sand filter improved as the filtration velocity increased and sand particle size decreased. On the other hand, Solé-Torres et al. (2019), using reclaimed effluents, observed higher turbidity removals at 30 m h^{-1} than at 60 m h^{-1}. Burt (2010) pointed out that most of the particles filtered are retained on the upper layer of the sand media bed despite the fact that some variation could be found depending on the filtration velocity and particle size. In this regard, De Deus, Testezlaf, & Mesquita, (2016), working with a 350 mm depth sand filter, found that finer media sizes (0.55 mm of effective diameter (d_e, i.e. sieve size opening that will pass through 10% of particles) promote upper (0–87.5 mm depth) particle retention rather than higher sizes (0.77 and 1.04 mm d_e). They also found that working at 75 m h^{-1} filtration velocity, more solids were retained at upper layers than 20 m h^{-1}. On the other hand, Ojha and Graham (1994), using numerical simulation in slow sand filters, found that after removing the 20–30 mm of the upper layer when the filter was clogged with particles, the filter was restored to having the head loss of a clean filter. In the same way, Rodgers et al. (2004) using 0.45 mm d_e sand, found that skimming the clogging layer to an approximate depth of 0.05 mm and replacing it with clean sand restored the filter field-saturated hydraulic conductivity. However, there are few studies focusing on how the particle retention is produced across the porous bed in pressurised media filters such as those used in drip irrigation systems. To carry out this approach, reliable procedures for measuring the particle retention across the filter media are needed. Van Staden and Haarhoff (2004) developed a methodology to determine the amount of total suspended solids (TSS) contained in the filtration media. It consists in taking a media from different depths and measuring the retained material, which is both time consuming and laborious. Therefore, other methods that could help analysing media filter performance may be of broader interest. Among these alternative procedures, those techniques that analyse images are particularly promising. However, most of the techniques for pore size distribution measurements are invasive and, therefore, destructive, expensive, relatively time-consuming, and/or they do not have sufficient resolution.

Optical coherence tomography (OCT), introduced by Huang et al. (1991), is based on an optical interference phenomena using broad-band light sources or frequency swept optical sources. Its main advantages are the rapid acquisition of multi-dimensional datasets, in-situ application and no requirement for sample preparation allowing for a non-invasive and complete characterisation of unaltered structures (Wagner & Horn, 2017). OCT has been mainly used in biomedicine with its first applications in ophthalmology focussing on retinal disease. Since then the technique has been adapted for the visualisation and quantification of biofouling in various media, for example in membrane filtration (Derlon et al., 2016; Fortunato et al., 2016) or drippers (Lequette, Ait-Mouheb & Adam et al., 2020, Lequette, Ait-Mouheb and Wery, 2020; Qian et al., 2017). The applications of OCT has also succeeded in revealing microstructures in porous media research, such as pore size and distribution (Campello et al., 2014). However, the penetration depth of OCT signal is limited to around 2 mm, which has restrained the application of this technique (Carrel et al., 2018).

The objective of this work is to assess the feasibility of using OCT to study fouling in pressurised media filter using RWW. There is also an intention to obtain quantitative data based on digital image processing. In this paper OCT fouling evaluations will be carried out at different depths.

2. Materials and methods

2.1. *Experimental setup*

A cylindrical polymethyl methacrylate (PMMA) media filter was designed and built (Fig. 1) for carrying out the experiments under laboratory conditions. Inner filter diameter was scaled down (by a factor of 4.54) from a commercial 500 mm diameter filter allowing experimentations to be carried out at laboratory level whilst keeping the same filtration water velocity. The use of filtration columns for testing the filter media performance is a common procedure provided the filtration

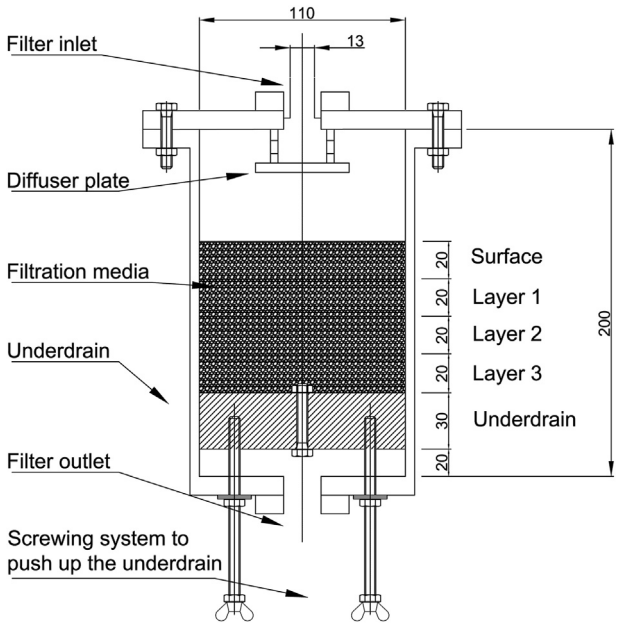

Fig. 1 – Experimental PMMA media filter. Dimensions are in mm.

velocity is respected For example, Rodgers et al. (2004) used 300 mm inner diameter column; Soyer et al. (2010) used a 110 mm inner diameter filtration column, and the Institut de la Filtration et des Techniques Séparatives (IFTS) tests media filters following the European standard (EN 16713–1:2016) in a 150 mm diameter columns. The filter used here had a 110 mm inner diameter (9503 mm^2 filtration surface), a diffuser plate was built to obtain a homogenous flow at the filter upper layer and, on the other end of the filter an iron-steel perforated plate was used as underdrain. In order to remove the media for analysis, a piston connected to a screw system was installed to raise the underdrain.

The experimental setup (Fig. 2) consisted of a 0.06 m^3 tank where the reclaimed effluent was placed, a digital water thermometer with an accuracy of ±1 °C, a centrifugal pump model TECNO-05/3 (ESPA, Banyoles, Spain), a water meter model 420 PC DN15 (Sensus, Raleigh, NC, USA) with an operational range from 0.016 to 3.12 $m^3\ h^{-1}$ and ±2% accuracy which allowed calculation of the superficial filtration velocity, and the PMMA media filter unit. Outlet and inlet filter pressures were measured using a digital manometer model Leo 2 (Keller, Winterthur, Switzerland) with a precision of ±0.07%. Target filtration velocity was achieved using a valve placed before the volume meter. The excess of the pumped water was returned to the effluent tank throughout the discharge pipe. With the regulation of the outflow valve, pressure at the filter inlet was adjusted to 100 kPa. A pressure relief valve was also installed. The purpose of this valve was to open automatically at a 200 kPa pressure to prevent any equipment failure. After being filtered, the effluent was returned to the tank, therefore the system worked as a closed circuit.

2.2. *Effluent used*

The reclaimed effluent from the wastewater treatment plant of Murviel-lès-Montpellier (Languedoc-Roussillon, France (43.605034° N, 3.757292° E)) was used. The wastewater treatment plant is designed around stabilisation ponds with three successive lagoons (13,680 m^3, 4784 m^3 and 2700 m^3, respectively) and a nominal capacity of 1500 inhabitants (equivalent).

Wastewater from the treatment plant was sampled weekly (24 samples collected through the season) in order to evaluate its water quality. Chemical oxygen demand (COD), ammonia, nitrate, and phosphorus concentrations were measured with a spectrophotometer (DR1900, Hach Company, Loveland, CO, USA) using Hach reagents®. Conductivity and pH were measured with probes (TetraCon® 925 and pH-Electrode

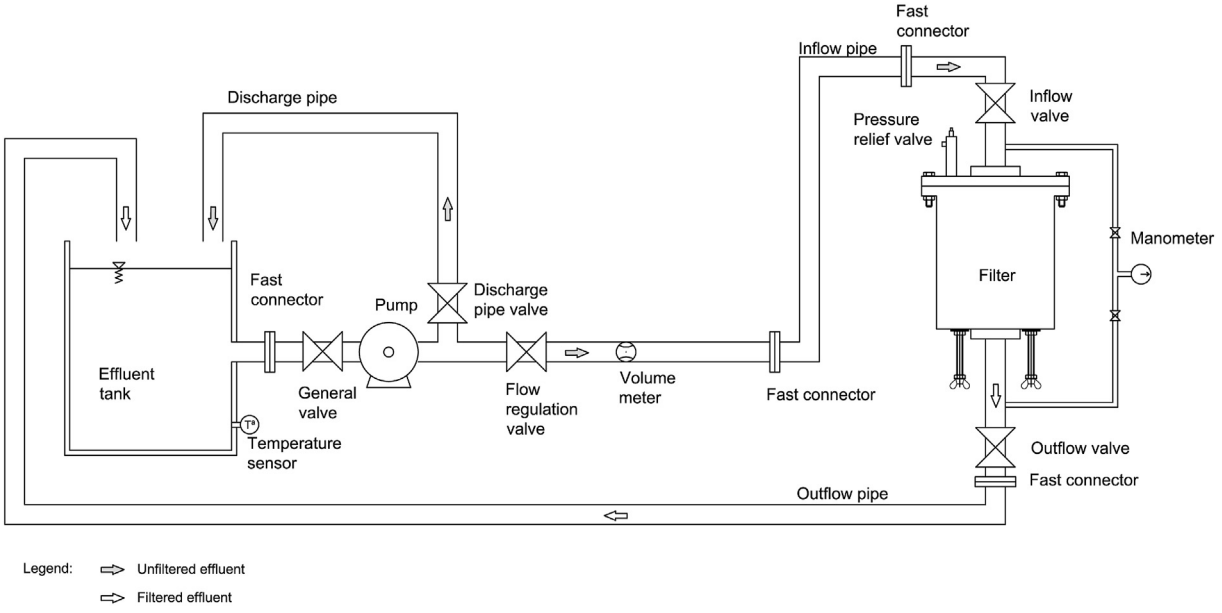

Fig. 2 – Diagram of the experimental setup.

Table 1 – Physico-chemical characteristics of the reclaimed wastewater during filtration experiments.

Parameter	Units	Mean and standard deviation (24 samples)
COD	g m^{-3}	70.3 ± 7.6
Ammonia	g m^{-3}	25.7 ± 7.8
Nitrate	g m^{-3}	0.7 ± 0.1
Phosphorus	g m^{-3}	4.9 ± 0.9
Electrical conductivity	μS cm^{-1}	1101.4 ± 51.5
Dissolved oxygen	g m^{-3}	6.8 ± 1.5
pH	–	6.9 ± 0.8

Sentix® 940, WTW, Wilhelm, Germany). The main effluent properties are listed in Table 1.

2.3. *Experimental procedure*

Even though silica sand is the most common filter media for micro irrigation (Nakayama et al., 2007), other materials such as recycled glass have been used because they exhibit similar or better filter removal efficiencies (Soyer et al., 2010), this option makes sense in particular in places where sans source are getting scarce. Thus, a commercial filtration media produced with clear glass, which presented a more homogeneous response at OCT observation than silica sand, was selected for this study. Two crushed recycled glass filtration media (Nature Works, L'Alfàs del Pi, Spain) were tested: NW1 with bulk density of 1189.08 kg m^{-3}, particle density of 2176.05 kg m^{-3}, d_e of 1.01 mm and porosity of 0.52; and NW2, with bulk density 1165.67 kg m^{-3}, particle density of 2107.35 kg m^{-3}, effective diameter of 0.75 mm and porosity of 0.54. Filter media characteristics were determined following Bové et al. (2015) methodology with each media having a bed height of 80 mm. Three filtration cycles for each condition were carried out, i.e. there were six experiments in total.

Before filling the filter with media, the apparatus was run for 3 min using tap water to clean it. Once the media was placed in the filter, backwashing was carried out for 3 min with tap water in order to remove the finest particles from the media. For the backwashing, an inflow pipe was placed at the filter outlet and an outflow pipe at the filter inlet, using fast connectors. After backwashing, the setup was drained and then the tank was filled with reclaimed effluent.

Fouling particles contained in the effluent from the wastewater treatment plant were used to clog the filter media. According to Bawiec and Pawęska (2020), particles in the outlet of a lagoon treatment are expected to be from 0.01 to 1000 μm. It is also reported that the particles which represent more than 75% of the particles volume had a mean particle diameter smaller than 100 μm. For each experiment, the tank was filled with 0.04 m^3 of the same day effluent sample and the trial was started adjusting the valves to get 25 m h^{-1} filtration velocity and 100 kPa filter inlet pressure. Filtered volume, inlet and outlet pressures (which allow calculating the head loss) and temperature were measured every 5 min. When the filter head loss increased by 50 kPa, the filtration test was considered finished. This threshold is usually taken as a target head loss to start the cleaning process of a media filter (Ravina et al., 1992). As the system worked in a closed-circuit and the particles in the effluent were removed by filtration, when head loss remained the same for 10 min (two measurements in a row), 0.01 m^3 of effluent from the tank were replaced for 0.01 m^3 of new effluent to maintain particle concentration in the experiment. In order to ascertain the variation of effluent characteristics during the filtration tests, water samples were taken at the beginning, before and after every effluent removal and at the end of the experiment. Main data of the experiment are presented at Table 2.

Total suspended solids concentration of the water samples were determined in the laboratory by gravimetry, after OCT acquisition (section 2.4), using 47 mm diameter and 1.2 μm pore glass microfiber filters. The inlet effluent differed from one test to another, as the samples for carrying out the experiments were taken on different days. Table 2 shows total suspended solids for the effluent at the beginning of the experiment for each condition and the mean of all the measurements during the experiment. Experiments were run with a wide range of initial water total suspended solids content, from 46.53 to 115.25 g m^{-3}. Using the TSS determined along a cycle and the filtered volume, which was recorded, the solid load of the filter was estimated, varying from 192.74 g to 513.86 g.

Retained particles in filtration media were determined following the procedure of van Staden and Haarhoff (2011), which needs a media sample from different depths with the aim of knowing the retention across the media bed. As it was previously described on section 2.1, a piston pushed up by a screw system was designed in order to push up the filtration media to allow taking slices of the filtration media. The total media depth (80 mm) was divided in four slices of 20 mm height each. After reaching the final head loss at each trial, each slice was carefully removed and put into a 1000 ml recipient. Further to this, 100 ml of distilled water was added, the recipient sealed and shake-inverted vigorously 5 times to achieve the physical stripping of the media, and the supernatant water was then decanted. This procedure was repeated 4 more times, so a total of 5 rounds per analysis were carried out and 500 ml of suspension was obtained, from which a sample of 50 ml was taken and then the TSS were determined. As all retained particles in the media had to pass through the 500 ml water solution (Haarhoff & van Staden, 2013), it was possible to calculate the mass of retained particles for each slice. On the other hand, each media slice was dried at 105 °C for 24 h and its weight determined with an AEJ 200-4CM (Kern & Sohn GmbH, Balingen, Germany) scale with an accuracy of ±0.1 mg, so the ratio between the mass of retained particles per mass of filtration media was known.

2.4. *Image sampling and analysis*

Once a filtration test was finished, the scaled filter was hermetically closed using both inlet and outlet valves, and the effluent was drained from the rest of the experimental set up, but not inside the filter. Filter was moved to another laboratory location, where images were taken using OCT image equipment. Three-dimensional OCT measurements were acquired using a Thorlabs GANYMEDE II OCT (LSM03 lens,

Table 2 – Averages ± standard deviation of the main parameters for each experiment.

Tested media	Initial effluent TSS (g m^{-3})	Total filtered volume (m^3)	Cycle duration (min)	Inlet pressure during the cycle (kPa)	Filtration velocity during the cycle (m h^{-1})	Added volume (m^3)	Estimated solid load during the cycle (g)	Effluent TSS mean during the cycle (g m^{-3})	Water temperature during the cycle (°C)
NW1	62.30	3.6	98	114 ± 0.21	23.93 ± 0.58	0.03	208.12	54.87 ± 6.47	25.81 ± 1.85
NW1	102.65	5.5	140	86 ± 0.19	25.93 ± 0.56	0.04	513.86	92.59 ± 10.50	25.84 ± 1.45
NW1	115.25	4.6	100	113 ± 0.06	23.97 ± 0.80	0.02	436.30	93.93 ± 16.34	26.05 ± 0.44
NW2	65.35	4.7	120	115 ± 0.09	24.25 ± 0.48	0.04	281.61	59.57 ± 7.71	27.10 ± 0.39
NW2	54.23	4.7	110	116 ± 0.09	24.27 ± 0.94	0.03	192.84	41.10 ± 8.72	26.60 ± 0.71
NW2	46.53	5.7	140	127 ± 0.13	25.08 ± 0.67	0.04	272.56	48.10 ± 5.62	24.85 ± 0.71

lateral resolution: 8 μm; Thorlabs GmbH, Lübeck, Germany). This lens provides a balanced lateral resolution, distance work and scanning area. The axial voxel size in water (n = 1.333) of GANYMEDE II was 2.1 μm and centre wavelength was 930 nm.

The filter was opened carefully, and the media pushed up with the screw system which helped the underdrain going up, as showed in Fig. 1. Once the media surface was placed at the top, images could be obtained. Effluent inside the filter was not removed, so the media was 1 mm below the filter top, and there was 1 mm height of effluent to allow a better OCT acquisition since there was not any change in the fouling form. As the media height was 80 mm, image sampling was divided into four slices, in order to determine fouling distribution across the depth. The OCT equipment was able to take images of the 2 mm upper depth of each slice. For each layer, six images of the top of each slice were taken following the same pattern. So, for every layer and filtration cycle, the same image samples were taken at the same locations (Fig. 3). For each cycle, a total of 24 images in 3D were taken (6 images per 4 layers). Once the images were taken, each filtration media layer of 20 mm was carefully removed and kept in 1000 ml receivers to determine the suspended solids retained, as was previously explained in section 2.3.

2.5. *Image processing*

Firstly, 3-D OCT datasets were processed in Fiji (running on ImageJ version 1.50b, Schindelin et al. (2009)). Secondly, an in-house code was used to detect the pixels associated with the fouling particles using MATLAB R2018r (MathWorks, Natick, MA, USA, version 2018b). A threshold (adapted to each dataset) was applied to digitise the dataset and the region above the threshold intensity losses during simple penetration. The intensity contrast between the fouling pixels and the remaining parts (transparent glass particles or water) was significant to allocate these last areas to the back-ground (black). Thus, in studied OCT acquisitions the threshold values vary between 0 and 60 with noise intensity between 0 and 15 (water and sand particles) and signal related fouling between 30 and 60. In addition, suspended solids and outliers were removed applying the 'clean and majority functions' of Matlab. For each position (x and y coordinates), the pixels associated with the fouling (up to the threshold) were summed (on the z coordinate) to obtain the fouling volume. Figure 4 illustrates the procedure used for the processing of OCT acquisitions.

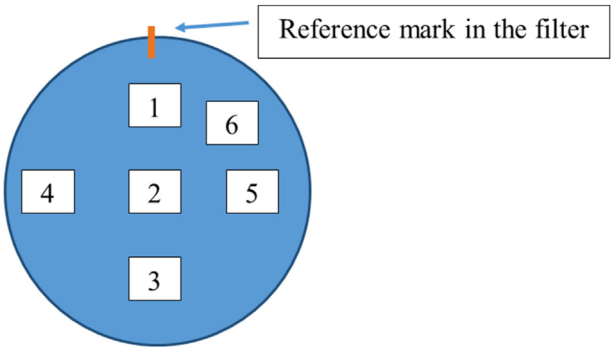

Fig. 3 – Section of the filter showing the order of the images taken with OCT.

In order to compare the level of fouling between filtration media particles, the fouling quantity was normalised by the pixel quantity of the corresponding measurement zones. The fouling coverage (%) was calculated for each measuring volume after data analysis according to Eq. (1):

$$\textit{Fouling coverage } \% = \frac{P_{fouling}}{P_{measurement\ zone}} \times 100 \quad (1)$$

Where $P_{fouling}$ is the number of pixels corresponding to retained particles from OCT acquisitions (pixels) and $P_{measurement\ zone}$ is the number of pixels of total OCT acquisitions of the sample determined by the taken image (pixels). There was not difference between 8 and 32 bits in the detail loss of OCT images and between the calculated coverage of the fouling results.

Then, for each layer image (corresponding to 2 mm depth), the mean value of the number of pixels corresponding to assessed retained particles was calculated, so one mean value was obtained per layer of each filtration cycle. It was possible to calculate the percentage of pixels regarding the total volume of the layer.

2.6. *Statistical analyses*

Tukey's mean separation test and regression statistical analyses were carried out using SPSS Statistics 25 software (IBM, Armonk, NY, USA) with a significance level of 0.05. Root mean square error (RMSE) was also computed to compare percentage of pixels and percentage of retained particles corresponding to each layer in the filtering media.

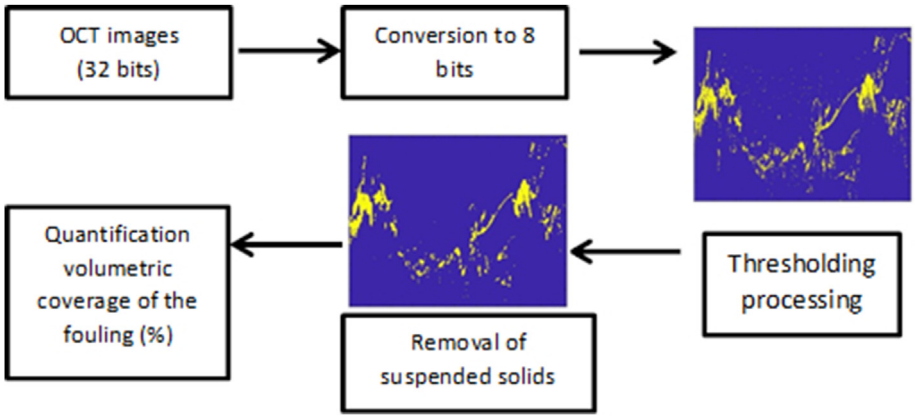

Fig. 4 – Image processing of OCT acquisition procedure.

3. Results and discussion

3.1. *Particle retention in media and image samplings*

Filter media particle retention across filter depth was determined using laboratory analysis and OCT image processing. Table 3 shows for each layer of the tested conditions, the results of the retained mass in the filtration media and the fouling coverage determined using image processing from the OCT as explained in section 2.3.

Higher particle retention was found in those conditions with more particle load at the beginning of the experiment (e.g. the cycle using NW1 with an initial load of 115.25 g [TSS] m^{-3}, compared with the cycle using NW2 with 46.53 g [TSS] m^{-3}). In general, there was a decrease of retained suspended solids as media depth increased, being the surface the layer which presented the most particle retention in all cases. Layer 3, located at the bottom, always presented less particle load, except for the cycle carried out with 115.25 g [TSS] m^{-3} using NW1, which was Layer 1. This test had the highest inlet TSS and was the second shortest cycle. The specific conditions of this cycle might have let that particles moved to the bottom of the filter bed. De Deus et al. (2016) working with a filtration velocity of 20 m h^{-1} and sand media size of d_e 1.04 mm (as NW1 media) also observed higher retention loads at the lower layers. Regarding pixel analysis, it was also the surface which presented most of the pixels in all the

Table 3 – Solid retention mass and number of megapixels for each tested condition tested.

Media	Effluent TSS (g m^{-3})	Slice	Depth (mm)	Relative dry weight of retained mass (mg g^{-1})	Dry weight of retained mass per layer (mg $layer^{-1}$)	Percentage of retained mass of the total (%)	Number of fouling pixels per layer	Fouling coverage percentage of the total (%)
NW1	62.30	Surface	0 to 20	1.48	362.27	35.29	1131	39.89
		Layer 1	20 to 40	1.09	259.60	25.29	680.	23.99
		Layer 2	40 to 60	0.99	226.17	22.03	804	28.36
		Layer 3	60 to 80	0.76	178.63	17.40	220	7.76
	102.65	Surface	0 to 20	2.00	482.53	33.27	1890	42.12
		Layer 1	20 to 40	2.07	417.27	28.77	1284	28.61
		Layer 2	40 to 60	1.92	376.93	25.99	881	19.64
		Layer 3	60 to 80	0.79	173.80	11.98	432	9.63
	115.25	Surface	0 to 20	3.06	789.50	40.15	2203	38.02
		Layer 1	20 to 40	1.70	349.64	17.78	849	14.65
		Layer 2	40 to 60	1.99	464.41	23.62	1348	23.26
		Layer 3	60 to 80	1.78	362.61	18.44	1394	24.06
NW2	65.35	Surface	0 to 20	1.06	203.87	31.81	2728	64.92
		Layer 1	20 to 40	0.82	165.00	25.74	449	10.70
		Layer 2	40 to 60	0.75	140.07	21.85	532	12.66
		Layer 3	60 to 80	0.73	132.00	20.59	492	11.72
	54.23	Surface	0 to 20	0.61	120.32	44.17	366	86.75
		Layer 1	20 to 40	0.50	87.54	32.14	32	7.67
		Layer 2	40 to 60	0.20	35.87	13.17	17	4.05
		Layer 3	60 to 80	0.14	28.65	10.52	6	1.52
	46.53	Surface	0 to 20	0.56	86.98	53.63	48	59.12
		Layer 1	20 to 40	0.21	35.28	21.75	21	26.47
		Layer 2	40 to 60	0.12	23.23	14.32	9	10.96
		Layer 3	60 to 80	0.09	16.68	10.29	2	3.45

cases, and layer 3 the least, except for NW1 and 115.25 g [TSS] m^{-3}, and NW2 and 65.35 g [TSS] m^{-3}, which was layer 1. In the same manner, the first 20 mm of filtration bed accumulated the highest percentage of retained particles, ranging from 33.27 to 53.63% in laboratory determination and from 38.02 to 86.75% in pixel assessment, while in the last layer (layer 3, from 60 to 80 mm) there was the lowest percentage of solid retention, ranging from 10.29 to 20.59%, and from 1.51 to 24.05% of TSS and pixel assessment, respectively. The highest retention in the first media layers was also observed by Burt (2010) and De Deus et al. (2016), using commercial media filters with tap water.

The percentage of pixels was correlated with that of retained particles for each layer for each experiment. Good correlations were obtained, with an R^2 ranging from 0.81 to 0.86 for NW1 media and from 0.69 to 0.97 for NW2. Root mean square error (RMSE) was acceptable when correlating NW1 media, with values between 3.39 and 5.57%, although with NW2 RMSE was higher (5.25–25.38%). The obtained correlation using all the data from all the experiments was slightly lower (R^2, 0.65) (Fig. 5). From the residual plot it can be concluded that the points were almost randomly dispersed around the axis, so the linear regression model could be appropriate for the data. In spite of this, from the relative error of the prediction by the range (Fig. 6 and Table 4) it could be said that for the 0–30% and 45–100% range, the prediction of the retained mass at the media, is slightly underestimated while for the 30–45% the prediction is slightly overestimated. Such results show that it is possible to establish a reasonable relationship between particles observed with OCT technique and processed with the total suspended solids retained in the media.

3.2. *Image media particle distribution*

Since, during OCT acquisition process, the same position was taken for all the replicates, it was possible to determine the percentage of the distribution of pixels for each location. As explained in section 2.5, not all the images were valid, so it was not possible to calculate the percentage of pixels for each location for all the repetitions. Statistical analysis was carried out to determine if the position was a significant factor for each layer taking into account all repetitions (Table 5). Factor location was not significant ($p > 0.05$) for the first three layers, meaning that there were no differences between the percentage of pixels among positions. For layer 3, at least one image for each condition was not valid, so it was not possible to determine the percentage of pixels for every location. Homogeneity in particle distribution discarded preferential water paths, which could affect filtration process and particle retention in media layers, meaning that experimental conditions were adequate to take valid measurements. Although preferential paths did not appear, the bed surface was not completely flat. This phenomenon was also observed by Mesquita et al. (2012), who saw excessive movement of the surface bed when working with filtration velocity values greater than or equal to 60 m h^{-1}. Surface bed movement could be mainly caused by an inadequate diffuser plate design, which causes irregular inlet flow distribution (Burt, 1994), increasing turbulence on the filtration surface (De Deus et al., 2016; Mesquita et al., 2019). The implemented diffuser plate, as mentioned above, was a prototype-sized whole filter, and maybe it could have caused some disturbance at filtration media surface.

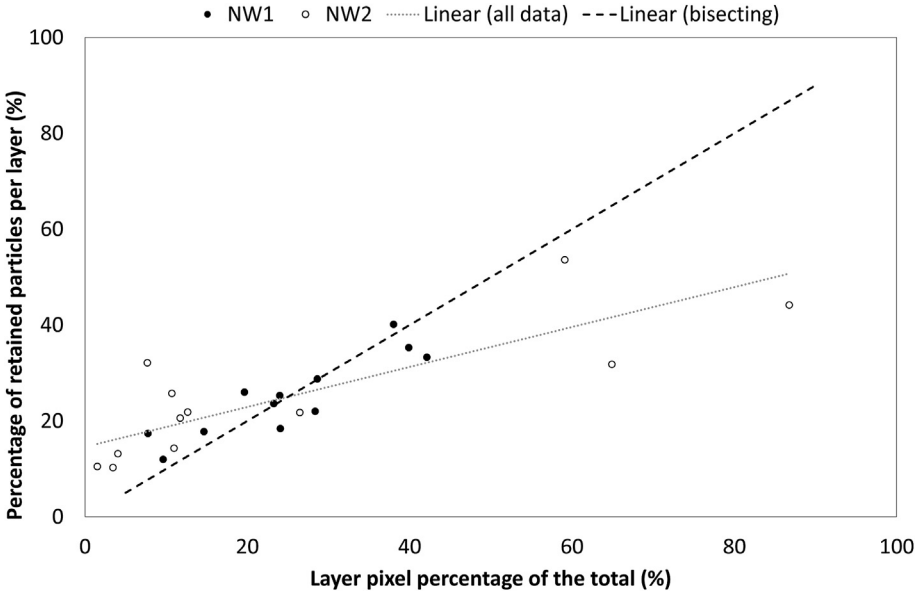

Fig. 5 – Correlation of the percentage of pixels and percentage of retained particles for the three repetitions carried out with both used media (NW1 and NW2). Correlation equation $y = 0.4166x + 14.584$ with $R^2 = 0.6573$ and $p < 0.05$.

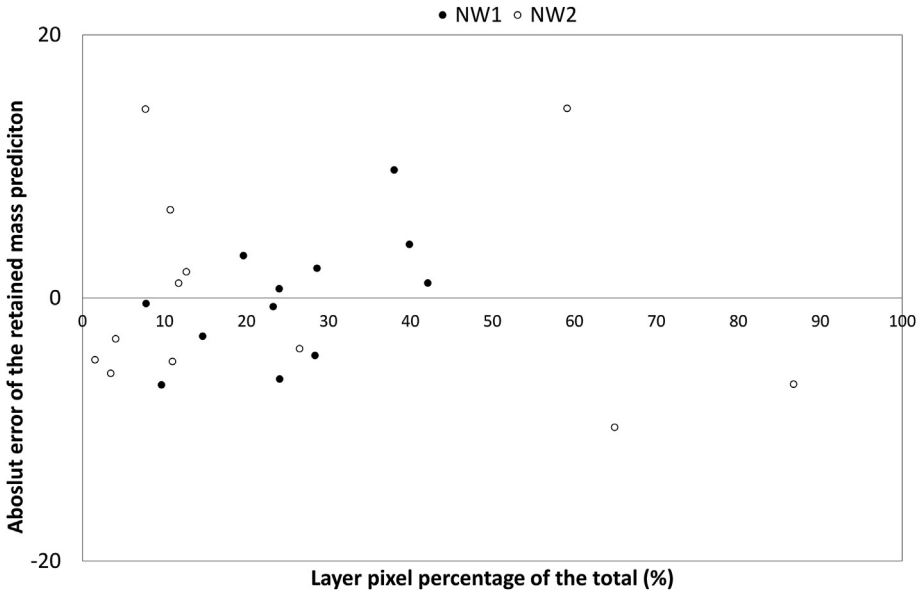

Fig. 6 – Residual plot of the predicted mass retained using the adjusted equation shown in Fig. 5 for all the cycles carried out with the media NW1 and NW2.

Table 4 – Mean and standard deviation of the relative error of the predicted value using the adjusted equation for measuring ranges.

Range of pixel layer measure (%)	Measurements (n)	Relative error (%)
0–15	11	−13.13 ± 33.10
15–30	7	−7.25 ± 17.56
30–45	3	5.45 ± 10.49
45–100	3	−6.26 ± 29.86

Table 5 – Number of valid observations and significance level of mean separation of factor location.

Slice	N	P-value
Surface	5	0.15
Layer 1	3	0.72
Layer 2	3	0.28
Layer 3	1	–

3.3. *Methodology limitations*

The proposed method entails limitations that must be taken into account given its complexity. On the one hand, during OCT acquisition, it is necessary to leave 1 mm of effluent at the top of the medium, to avoid reflections. In addition, the OCT measurement surface is limited to approximately 100 mm 2 thus it would be difficult to sample a real sized media filter with filtration surface higher than 1.5 m^2. For each layer (20 mm depth), the fouling thickness using OCT is only detected in a maximum of 2 mm media depth, which would impose tighter layers to follow the detailed deposition kinetics.

On the other hand, screw underdrain lift system can influence and move the retained particles in the different layers, affecting the result. Finally, slice removing for the determination of the retention of solids is demanding laboratory work which is also a critical step that can affect the process error.

In addition, although OCT detects reflection and scattering signals, it is well suited to visualise the overall distribution of particular matter in biofilms which commonly appear in wastewater filtration. However, it seems difficult to reproduce our optical methodology in the case of retention volume quantification by inorganic particles (sands for example), because these solid particles will naturally reflect the signal.

4. Conclusions

Optical coherence tomography (OCT) is a technique that could be used to analyse and quantify fouling retention at different depths and location in media filters used in drip irrigation systems. The results obtained show that by using OCT and its data analysis, as well as experimental total solid determination, it is possible to quantify the retained mass of particles in a filtration media. For assayed experimental conditions and with the used clogging particles, in this case from a treated wastewater, the obtained linear equation to predict the retained mass presented a significant ($p < 0.05$) regression coefficient $R^2 = 0.657$. The minimum relative error (around 5.5%) was obtained when the layer pixel attributed to particles was between 30 and 45% and reached its maximum (about 13%) when the layer pixel was below 15%.

However, further research should be carried out, concerning filtration conditions and measurement process, for validating the procedure, especially at a commercial filter scale. For the former, different media heights and filtration velocities should be tested. Overall, OCT appears a good and feasible tool to quantify particle retention across media filters, to study the particle distribution across them, and to identify preferential circulation in the media filters. The main

drawback of this technique is that requires to analysis of filter media using thin slices.

Declaration of competing interest

The authors declare that they have no known competing financial interests or personal relationships that could have appeared to influence the work reported in this paper.

Acknowledgements

The authors would like to express their gratitude to Spanish Research Agency and the European Regional Development Fund for their financial support through Grant RTI2018-094798-B-100. They also want to thank the University of Girona for funding the research stages of Miquel Duran-Ros and Carles Solé-Torres at INRAE Montpellier (France). The authors also gratefully acknowledge the financial support of the French Water Agency Rhône Méditerranée Corse, project "Experimental platform for the reuse of reclaimed wastewater in irrigation, Murviel-lès-Montpellier".

REFERENCES

Ait-Mouheb, N., Bahri, A., Thayer, B. B., Benyahia, B., Bourrié, G., Cherki, B., … Harmand, H. (2018). The reuse of reclaimed water for irrigation around the mediterranean rim: A step towards a more virtuous cycle? *Reginal Environmental Change, 18*, 693–705. https://doi.org/10.1007/s10113-018-1292-z

Awady, M. N. E., El Berry, A. M., Genaidy, M. A. I., & Zayton, A. M. (2008). Mathematical model for predicting the performance of trickle irrigation system. *Misr Society of Agricultural Engineering - Irrigation and Drainage, 25*, 837–860.

Ayars, J. E., Bucks, D. A., Lamm, F. R., & Nakayama, F. S. (2007). Introduction. In F. R. Lamm, J. E Ayars, & F. S. Nakayama (Eds.), *Microirrigation for crop production. Design, operation, and management* (pp. 1–26). Amsterdam: Elsevier.

Bawiec, A., & Pawęska, K. (2020). Changes in the granulometric composition of particles in wastewater flowing through a hydroponic lagoon used as the third stage in a wastewater treatment plant. *Water Science and Technology, 81*(9), 1863–1869. https://doi.org/10.2166/wst.2020.235

Bové, J., Arbat, G., Duran-Ros, M., Pujol, T., Velayos, J., Ramírez de Cartagena, F., et al. (2015). Pressure drop across sand and recycled glass media used in micro irrigation filters. *Biosystems Engineering, 137*, 55–63. https://doi.org/10.1016/j.biosystemseng.2015.07.009

Burt, C. M. (1994). Media tanks for filtration. Part I. Tank sizing and media selection. *Irrigation Journal, 44*(5), 14–17.

Burt, C. M. (2010). Hydraulics of commercial sand media filter tank used for agricultural drip irrigation. *Irrigation and Drainage Systems*. Report Nº R 10001. San Luis Obispo, CA, USA.

Burt, C. M., & Styles, S. W. (2016). *Drip and micro irrigation for trees, vines, and row crops* (5th ed.). San Luis Obispo, California: ITRC.

Campello, S. L., Santos, W. P., Machado, V. F., Mota, C. C. B. O., Gomes, A. S. L., & de Souza, R. E. (2014). Micro-structural information of porous materials by optical coherence tomography. *Microporous and Mesoporous Materials, 198*, 50–54. https://doi.org/10.1016/j.micromeso.2014.07.009

Carrel, M., Morales, V. L., Beltran, M. A., Derlon, N., Kaufmann, R., Morgenroth, E., et al. (2018). Biofilms in 3D porous media: Delineating the influence of the pore network geometry, flow and mass transfer on biofilm development. *Water Research, 134*, 280–291. https://doi.org/10.1016/j.watres.2018.01.059

De Deus, F. P., Testezlaf, R., & Mesquita, M. (2016). Assessment methodology of backwashing in pressurised sand filters. *Revista Brasileira de Engenharia Agrícola e Ambiental, 20*(7), 600–605. https://doi.org/10.1590/1807-1929/agriambi.v20n7p600-605

Derlon, N., Grutter, A., Brandenberger, F., Sutter, A., Kuhlicke, U., Neu, T. R., et al. (2016). The composition and compression of biofilms developed on ultrafiltration membranes determine hydraulic biofilm resistance. *Water Research, 102*, 63–72. https://doi.org/10.1016/j.watres.2016.06.019

EN 16713-1. (2016). *Domestic swimming pools – water systems – Part 1: Filtration systems- Requirements and tests methods*.

EPA. (1995). *Water treatment manual*. Wexford: Environmental Protection Agency.

Fortunato, L., Jeong, S., Wang, Y., Behzad, A. R., & Leiknes, T. (2016). Integrated approach to characterise fouling on a flat sheet membrane gravity driven submerged membrane bioreactor. *Bioresource Technology, 222*, 335–343. https://doi.org/10.1016/j.biortech.2016.09.127

Haarhoff, J., & van Staden, S. J. (2013). Measurement and expression of granular filter cleanliness. *WaterSA, 39*(5), 701–706.

Huang, D., Swanson, E. A., Lin, C. P., Schuman, J. S., Stinson, W. G., Chang, W., … Fujimoto, J. G. (1991). Optical coherence tomography. *Science, 254*(5035), 1178–1181. https://doi.org/10.1126/science.1957169

Lamm, F. R., & Rogers, D. H. (2017). Longevity and performance of a subsurface drip irrigation system. *Transactions of the ASABE, 60*(3), 931–939. https://doi.org/10.13031/trans.12237

Lazarova, V., & Bahri, A. (2004). *Water reuse for irrigation. Agriculture, landscapes, and turf grass*. Boca Raton: CRC Press.

Lequette, K., Ait-Mouheb, N., Adam, N., Muffat-Jeandet, M., Bru-Adan, V., & Wéry, N. (2020). Effects of the chlorination and pressure flushing of drippers fed by reclaimed wastewater on biofouling. *Sience of the Total Environmnet*. https://doi.org/10.1016/j.scitotenv.2020.143598. *In press*, art. 143598.

Lequette, K., Ait-Mouheb, N., & Wery, N. (2020). Hydrodynamic effect on biofouling of milli-labyrinth channel and bacterial communities in drip irrigation systems fed with reclaimed wastewater. *The Science of the Total Environment, 738*, 139778. https://doi.org/10.1016/j.scitotenv.2020.139778. art.

Mesquita, M., de Deus, F., Testezlaf, R., da Rosa, L., & Diotto, A. (2019). Design and hydrodynamic performance testing of a new pressure sand filter diffuser plate using numerical simulation. *Biosystems Engineering, 183*, 59–69. https://doi.org/10.1016/j.biosystemseng.2019.04.015

Mesquita, M., Testezlaf, R., & Ramirez, J. (2012). The effect of media bed characteristics and internal auxiliary elements on sand filter head loss. *Agricultural Water Management, 115*, 178–185. https://doi.org/10.1016/j.agwat.2012.09.003

Nakayama, F. S., Boman, B. J., & Pitts, D. J. (2007). Maintenance. In F. R. Lamm, J. E Ayars, & F. S. Nakayama (Eds.), *Microirrigation for crop production. Design, operation, and management* (pp. 389–430). Amsterdam: Elsevier.

Ojha, C. S. P., & Graham, N. J. D. (1994). Computer-Aided simulation of slow sand filter performance. *Water Research, 28*(5), 1025–1030. https://doi.org/10.1016/0043-1354(94)90187-2

Puig-Bargués, J., Barragán, J., & Ramírez de Cartagena, F. (2005). Filtration of effluents for microirrigation systems. *Transactions*

of the ASABE, 48(3), 968–978. https://doi.org/10.13031/2013.18509

Qian, J., Horn, H., Tarchitzky, J., Chen, Y., Katz, S., & Wagner, M. (2017). Water quality and daily temperature cycle affect biofilm formation in drip irrigation devices revealed by optical coherence tomography. *Biofouling*, *33*(3), 211–221. https://doi.org/10.1080/08927014.2017.1285017

Ravina, I., Paz, E., Sofer, Z., Marcu, A., Shisha, A., & Sagi, G. (1992). Control of emitter clogging in drip irrigation with reclaimedwastewater. *Irrigation Science*, *13*(3), 129–139. https://doi.org/10.1007/BF00191055

Rodgers, M., Mulqueen, J., & Healy, M. G. (2004). Surface clogging in an intermittent stratified sand filter. *Soil Science Society of America Journal*, *68*(6), 1827–1832. https://doi.org/10.2136/sssaj2004.1827

Schindelin, J., Arganda-Carrera, I., Frise, E., Verena, K., Mark, L., Tobias, P., … Albert, C. (2009). Fiji - an open platform for biological image analysis. *Nature Methods*, *9*(7), 676–682. https://doi.org/10.1038/nmeth.2019

Solé-Torres, C., Puig-Bargués, J., Duran-Ros, M., Arbat, G., Pujol, J., & Ramírez de Cartagena, F. (2019). Effect of underdrain design, media height and filtration velocity on the performance of mircroirrigation sand filters using reclaimed effluents. *Biosystems Engineering*, *187*, 292–304. https://doi.org/10.1016/j.biosystemseng.2019.09.012

Soyer, E., Akgiray, Ö., Eldem, N.Ö., & Saatçi, A. M. (2010). Crushed recycled glass as a filter medium and comparison with silica sand. *Clean - Soil, Air, Water*, *38*(10), 927–935. https://doi.org/10.1002/clen.201000217

van Staden, S. J., & Haarhoff, J. (2004). A standard test for filter media cleanliness. *WaterSA*, *30*(1), 81–88. https://doi.org/10.4314/wsa.v30i1.5030

van Staden, S. J., & Haarhoff, J. (2011). The use of filter media to determine filter cleanliness. *Physics and Chemestry of the Earth*, *36*, 1135–1140. https://doi.org/10.1016/j.pce.2011.07.067

Trooien, T. P., & Hills, D. J. (2007). Application of biological effluent. In F. R. Lamm, J. E. Ayars, & F. S. Nakayama (Eds.), *Microirrigation for crop production. Design, operation and management* (pp. 329–356). Amsterdam: Elsevier.

Wagner, M., & Horn, H. (2017). Optical coherence tomography in biofilm research: A comprehensive review. *Biotechnology and Bioengineering*, *114*(7), 1386–1402. https://doi.org/10.1002/bit.26283

WHO. (2006). *Guidelines for the safe use of wastewater, excreta and greywater* (Vol. 2). Geneva: World Health Organization Press.